Journal of King Saud University – Engineering Sciences (2018) 30, 355–362

King Saud University

Journal of King Saud University – Engineering Sciences

www.ksu.edu.sa
www.sciencedirect.com

ORIGINAL ARTICLES

Exergy based modeling and optimization of solar thermal collector provided with impinging air jets

Ranchan Chauhan [a,*], **N.S. Thakur** [b], **Tej Singh** [c], **Muneesh Sethi** [a]

[a] *Faculty of Engineering and Technology, Shoolini University, Solan, HP 173229, India*
[b] *Centre for Energy and Environment, NIT Hamirpur, HP 177005, India*
[c] *Department of Mechanical Engineering, Manav Bharti University, Solan, HP 173229, India*

Received 12 March 2016; accepted 12 July 2016
Available online 9 August 2016

KEYWORDS

Solar thermal collector;
Jet impingement;
Exergy;
Heat transfer;
Optimization

Abstract The irreversible absorption of solar energy accompanied by emission for conversion into thermal energy takes place at the cost of exergy losses from the collector and the effectiveness of this conversion is evaluated in terms of exergy efficiency based upon second law of thermodynamics. Presented in this paper is the exergetic efficiency of impinging jet solar thermal collector and its comparison with that of conventional solar collector. The effect of flow Reynolds number, jet diameter, streamwise and spanwise pitch between the jets on exergetic efficiency of impinging jet solar air collector during conversion of solar energy into thermal energy has been studied based upon the correlations developed for heat transfer coefficient and friction factor in the range of investigated flow and geometric parameters. The results reveal that the impinging air jets extract the absorbed exergy from the absorber to the air flowing beneath with higher efficiency than that of the conventional solar air collector. Also, the design plots have been prepared for jet plate parameters with temperature rise parameter in order to obtain an optimum parameter values that would deliver maximum exergetic efficiency for desired value of temperature rise. Design procedure has also been discussed to evaluate the optimum parameters with respect to operating conditions.
© 2016 The Authors. Production and hosting by Elsevier B.V. on behalf of King Saud University. This is an open access article under the CC BY-NC-ND license (http://creativecommons.org/licenses/by-nc-nd/4.0/).

1. Introduction

The thermal conversion process of solar energy is based upon the well known phenomenon of heat transfer. Solar energy utilization system is used to trap the available solar energy and convert it into useful forms depending upon the need (Raju and Narayana, 2018; Chauhan et al., 2016; Panchal, 2015; Krishnananth and Murugavel, 2013; Almasoud and Gandayh, 2015; Alaudeen et al., 2014). The efficiency of the solar energy utilization system depends upon the solar insolation; the degree to which the sunlight is concentrated; measures taken to reduce the heat losses from the system and the heat transfer phenomenon through which the heat is transferred to the working fluid. Solar air collector is a simplest form of solar energy conversion system in which the solar radiation

* Corresponding author. Fax: +91 1792 308000.
E-mail address: ranchanc85@gmail.com (R. Chauhan).
Peer review under responsibility of King Saud University.

Production and hosting by Elsevier

http://dx.doi.org/10.1016/j.jksues.2016.07.003
1018-3639 © 2016 The Authors. Production and hosting by Elsevier B.V. on behalf of King Saud University.
This is an open access article under the CC BY-NC-ND license (http://creativecommons.org/licenses/by-nc-nd/4.0/).

energy is transformed into thermal energy which is extracted by the air flowing under the absorbing surface.

The commercial viability of solar air collectors mainly depends upon their thermal performance and cost effectiveness with most studies suggesting that the key parameter to enhance the solar collector performance is the rate of heat transfer between the solar energy absorbing surface and the flowing air (Kumar and Rosen, 2011). The information regarding its thermal efficiency is useful for existing and projected future solar energy system design methods. The solar air collectors are generally used for low and moderate temperature requirements such as supplying hot air to buildings, agricultural and industrial drying etc. (Bansal, 1999). Numerous studies have been reported in the literature for heat transfer enhancement in solar air collectors (Shokouhmand et al., 2009; Al-Dabbas, 2015; Chauhan and Thakur, 2014). Impinging air jets helps in increasing the thermal performance of solar collector by increasing the convective heat transfer coefficient from heated absorber surface to the air impinging over it. Impinging air jets released against the heat transferring surface transfer large amount of thermal energy as the impingement boundary layers are much thinner and also the spent fluid after impingement serves to turbulate the surrounding fluid (Zuckerman and Lior, 2006). The other heat transfer applications where jet impingement has proved its superiority are turbine blades (Han, 2004), micro-channel chip cooling (Kandlikar and Bapat, 2007), solar heat absorbers (Roger et al., 2005) etc. Heat transfer using impinging air jets has received considerable research attention in recent years due to high heat transfer rates that occurs in the impingement region and is an active area of research (Meola, 2009).

However, the literature is found deficient with exergetic optimization studies related to solar air collector provided with impinging air jets. Since, it is desirable that high rates of heat transfer achieved using jet impingement should employ minimum power requirement for propelling the air through the collector duct, therefore the exergy based optimization has been employed for this purpose in order to evaluate by what means is impinging jet solar air collector cost effective than the conventional air collector. The method of exergy analysis is regarded as an essential tool for predicting the solar collector performance as it measures the maximum work potential a system can deliver with minimum energy input. This study therefore presents second law optimization in terms of exergetic efficiency of impinging jet solar air collector which takes into account the pumping power required to maintain the desired flow rate through the collector duct with simultaneous consideration over the useful heat energy extracted by convection mechanism. The effect of different jet plate parameters viz. jet diameter, streamwise and spanwise pitch each normalized by the hydraulic diameter of the duct on exergetic efficiency has been carried out along with conventional solar collector. Based upon the results, design plots for each jet plate parameter have been plotted and also design procedure has been discussed in order to arrive at optimum value of jet parameters for desired value of temperature rise.

2. Exergy analysis

The first law efficiency is a common measure of energy use efficiency concerned with quantity of energy and disregards the form in which energy exists. The second law provides a means of assigning a quality index to energy. Exergy analysis is an assessment technique for systems and processes based upon the second law of thermodynamics and defined as the maximum work potential which can be obtained from a form of energy (Bejan, 1988). The irreversibilities such as friction, heat transfer through a finite temperature difference, mixing, non-quasi-equilibrium compression or expansion always generate entropy and anything that generates entropy always destroys exergy. The exergy destroyed represents the lost work potential and is also called the irreversibility or lost work (Cengel and Boles, 2008). Exergy analysis yields useful results as it deals with irreversibility minimization or maximum exergy delivery, thereby ensuring the most efficient possible conversion of energy for the required task (Lior and Zhang, 2007). Exergy analysis has proved to be a powerful tool in the thermodynamic analysis of energy systems.

The exergy flow diagram of solar air collector is as shown in Fig. 1. The measure of quality of energy involved in a solar collector can be accounted by incorporating the quality of useful energy output and frictional losses along with the other losses occurring inside the solar collector duct. Altfeld et al. (1988) proposed a method based upon second law of thermodynamics for establishing the equivalence of useful energy output and frictional losses in solar air collector. The exergetic efficiency can be expressed as:

$$\eta_{exr} = E_n / E_s \tag{1}$$

In the above equation, the net exergy flow is the increase of exergy flow of air while flowing through the collector and is to be maximized for optimization. The exergy flow is defined as:

$$E_n = I A_p \eta_{th} \eta_c - P_m (1 - \eta_{ct}) \tag{2}$$

The first term on the right side of Eq. (2) represents the exergy of absorbed solar energy which is transferred to the flowing air and the second term represents the exergy losses due to friction. The exergy losses due to absorption of irradiation are high enough and also the losses due to heat transfer to fluid, heat transfer to environment and losses due to friction impacts the exergy transfer to the working fluid. The exergy inflow associated with solar irradiation on the surface of the solar collector is given by:

$$E_s = I \times A_p (1 - T_a / T_{sun}) \tag{3}$$

Substituting the values of (E_n) and (E_s) from Eq. (2) and Eq. (3) in Eq. (1), the exergetic efficiency can be computed. As in the Eq. (1) the term in the denominator is constant, thus the exergetic efficiency of the system can be maximized by maximizing the numerator term (E_n) which can be done by minimizing the exergy losses taking place in solar air collector.

3. Mathematical approach

The mathematical model used for computation of the performance of impinging jet solar thermal collector has been discussed to study the variation of flow and geometrical parameters on exergetic efficiency. The important assumptions considered are: steady state condition; negligible heat conduction in the flow direction; negligible edge effects. The range of parameters has been selected based upon the experimental investigation (Chauhan and Thakur, 2013). The performance

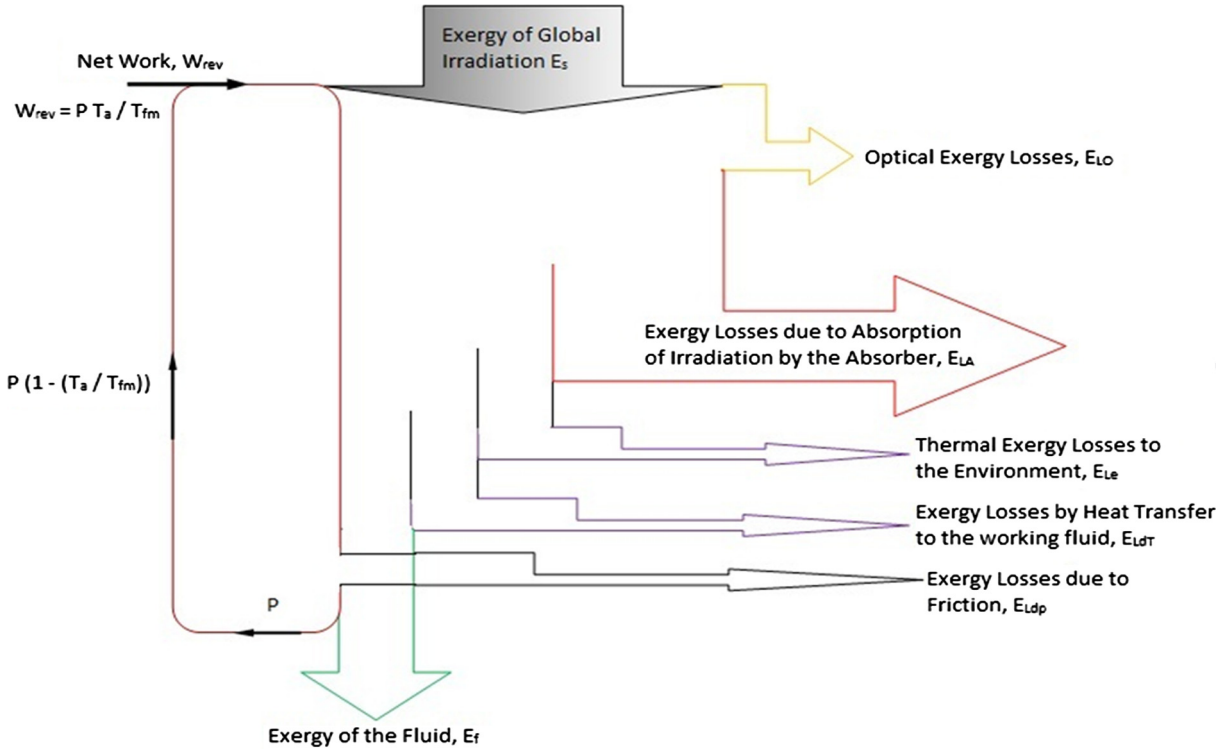

Figure 1 Exergy flow diagram of solar thermal collector.

and optimization has been carried out as a function of two basic design parameters, namely: temperature rise parameter, $[\Delta T/I]$ and solar insolation, (I). The range of both these design parameters has been decided based upon the range of application of solar air collectors. The procedure for computation of exergetic efficiency is discussed below:

Step 1: The parameters such as collector dimensions, inlet temperature, wind speed etc. are set fixed and the varying parameters such as jet plate parameters as shown in Table 1 are selected accordingly for computation of performance.

Table 1 Range of flow and geometrical parameters.

Input Data	Numerical Value(s)
System parameters	
Collector dimensions ($L \times W \times H$)	$1.4 \times 0.29 \times 0.025$ m
Emissivity of absorber plate, (ε_p)	0.9
Emissivity of glass cover, (ε_g)	0.88
Jet diameter ratio (D_j/D_h)	0.043–0.109
Number of glass covers (N)	1
Streamwise pitch ratio (X/D_h)	0.435–1.739
Spanwise pitch ratio (Y/D_h)	0.435–0.869
Transmittance-Absorptance ($\tau\alpha$)	0.8
Operating parameters	
Reynolds number (Re)	3500–25,000
Wind velocity (V_w) m/s	1 m/s
Ambient temperature (T_a), K	300 K
Solar radiation intensity (I), W/m^2	500–1000 W/m^2

Step 2: The hydraulic diameter of the duct and the area of the absorber surface are calculated as:

$$D_h = \frac{4 \times (W \times H)}{2 \times (W + H)}; A_p = W \times L \tag{4}$$

Step 3: The temperature of outlet air is computed from the temperature rise of air and inlet air temperature. The fluid mean temperature is then calculated as the mean of both the temperature.

Step 4: The specific heat of air, dynamic viscosity and thermal conductivity of air are calculated using following relations:

$$C_p = 1006\left(\frac{T_{fm}}{293}\right)^{0.0155}; \ \mu = 1.81 \times 10^{-5}\left(\frac{T_{fm}}{293}\right)^{0.735}; \ k = 0.0257 \times \left(\frac{T_{fm}}{293}\right)^{0.86} \tag{5}$$

Step 5: Initially the temperature of the absorber plate is approximated to be as:
$T_{pm} = T_{fm} + 10$

Step 6: Based upon this approximation, the overall heat loss coefficient is calculated which is the sum of top, bottom and edge loss coefficients. The overall heat loss coefficient is given as:

$U_L = U_t + U_b + U_e$
The top loss, the edge loss and the bottom loss coefficients are expressed as follows:

The top loss (Klein, 1975);

$$U_t = \left[\frac{N}{\frac{c_t}{T_{pm}}\left(\frac{T_{pm}-T_a}{N+f_t}\right)^{0.33}} + \frac{1}{h_w}\right]^{-1} + \left[\frac{\sigma(T_{pm}^2 + T_a^2)\ (T_{pm}+T_a)}{\frac{1}{(\in_P + 0.05\times N(1-\in_P))} + \frac{2\times N + f_t - 1}{\in_g} - 1}\right] \quad (6)$$

The edge loss and bottom loss are calculated according to following relations;

$$U_e = \frac{(W+L)\times L_1 \times k_i}{W \times L \times t_e}; \quad U_b = \frac{k_i}{t_i} \quad (7)$$

Step 7: The useful heat gain, mass flow rate and the flow Reynolds number as calculated as:

$$Q_{u1} = [I(\tau\alpha) - U_L(T_{pm} - T_a)] \times A_p;$$
$$\dot{m} = \frac{Q_{u1}}{C_p \times \Delta T};\ \mathrm{Re} = \frac{G \times D_h}{\mu_a} \quad (8)$$

Step 8: The Nusselt number is calculated by the correlation reported in literature (Chauhan and Thakur, 2013) for impinging jet solar air collector:

$$Nu = 1.658\times 10^{-3}\mathrm{Re}^{0.8512}(X/D_h)^{0.1761}(Y/D_h)^{0.141} \times (D_j/D_h)^{-1.9854} \times \exp[-0.3498(\ln(D_j/D_h))^2] \quad (9)$$

Step 9: The collector heat removal factor, F_R and the plate efficiency factor, F' are computed as (Duffie and Beckman, 1974):

$$F_R = \frac{\dot{m}\times C_p}{A_p \times U_L}\left[1 - \exp\left(-\frac{A_p U_L F'}{\dot{m} C_p}\right)\right];\ F' = \frac{h}{h + U_L} \quad (10)$$

where h is the heat transfer coefficient and is calculated as: $h = \frac{Nu\times k}{D_h}$.

Step 10: The new value of useful heat gain is then calculated from the collector heat removal factor as:

$$Q_{u2} = F_R \times A_p[I(\tau\alpha) - U_L(T_{fi} - T_a)] \quad (11)$$

The value of Q_{u1} obtained from Eq. (8) and value of Q_{u2} obtained from Eq. (11) are compared. If the two values differ by 0.1%, then the plate temperature is modified as:

$$T_{pm} = T_a + \left[\frac{\{I(\tau\alpha) - \frac{Q_{u2}}{A_p}\}}{U_L}\right] \quad (12)$$

This new temperature of the absorber plate is used and the calculations are performed again till the difference between the two values of useful heat gain is below 0.1% of Q_{u1}.

Step 11: The thermal efficiency is calculated from useful heat gain as:

$$\eta_{th} = Q_u/I \times A_p \quad (13)$$

Step 12: The friction factor is calculated by the correlation reported for impinging jet solar air collector and is reproduced below for ready reference (Chauhan and Thakur, 2013):

$$f = 0.3475\mathrm{Re}^{-0.5244}(X/D_h)^{0.4169}(Y/D_h)^{0.5321}(D_j/D_h)^{-1.4848} \times \exp[-0.221(\ln(D_j/D_h))^2] \quad (14)$$

Step 13: Using this correlation for friction factor, the pressure drop and the mechanical power required to drive the air through the duct are calculated using following relations:

$$(\Delta P)_d = \frac{2fLG^2}{\rho_a \times D_h}; \quad P_m = \frac{\dot{m}\times(\Delta P)_d}{\rho_a} \quad (15)$$

Step 14: Finally, the exergetic efficiency is computed using Eq. (1) for the set of system and operating parameters. The calculations are repeated to cover the entire range of the parameters.

4. Results and discussion

The exergetic efficiency is computed to study the effect of jet plate parameters and flow Reynolds number in an impinging jet solar air collector using the mathematical model discussed above. Fig. 2a and b shows the variation of η_{exr} and η_{th} with (Re) and $[\Delta T/I]$ at (D_j/D_h) of 0.065; (X/D_h) of 1.739 and (Y/D_h) of 0.869. It can be seen from Fig. 2a that the η_{th} increases with increase in (Re) whereas the η_{exr} first increases and then starts decreasing. The increase in η_{th} is due to increase in useful heat gain and also increase in (Re) increases turbulence which increases heat transfer coefficient from absorber to the air flowing beneath. The η_{exr} of impinging jet solar air collector first increases at lower (Re) range and then starts decreasing with further increase in (Re). The decrease in η_{exr} with (Re) is attributed mainly because of exergy losses that take place in the collector duct. The most important exergy loss results from the absorption of solar irradiation at mean temperature (Altfeld et al., 1988). The high temperature of the absorber surface reduces the exergy losses due to absorption but increases the thermal losses to the environment. The variation of exergy loss components is discussed by Singh et al. (2012). It is evident that at higher values of (Re) the pumping power requirement dominates the useful heat gain due to which the net exergy flow from the solar air collector becomes negative and thus it is desirable to operate the system at low (Re) range for maximum η_{exr}.

The effect of jet plate parameters on η_{exr} with $[\Delta T/I]$ has been evaluated as shown in Fig. 3a–c. Fig. 3a shows the effect of (D_j/D_h) on η_{exr} with $[\Delta T/I]$ at (X/D_h) of 1.739 and (Y/D_h) of 0.869. As seen from the figure, the conventional solar collector delivers higher η_{exr} at low values of $[\Delta T/I]$. For $[\Delta T/I]$ higher than 0.012 km^2/W, the value of (D_j/D_h) of 0.065 have the highest η_{exr} and for $[\Delta T/I]$ below 0.012 km^2/W, η_{exr} is function of (D_j/D_h) having different values.

This variation in exergetic efficiency due to variation in (D_j/D_h) is due to variation in the level of interference between the adjacent jets prior to impingement which commonly deter-

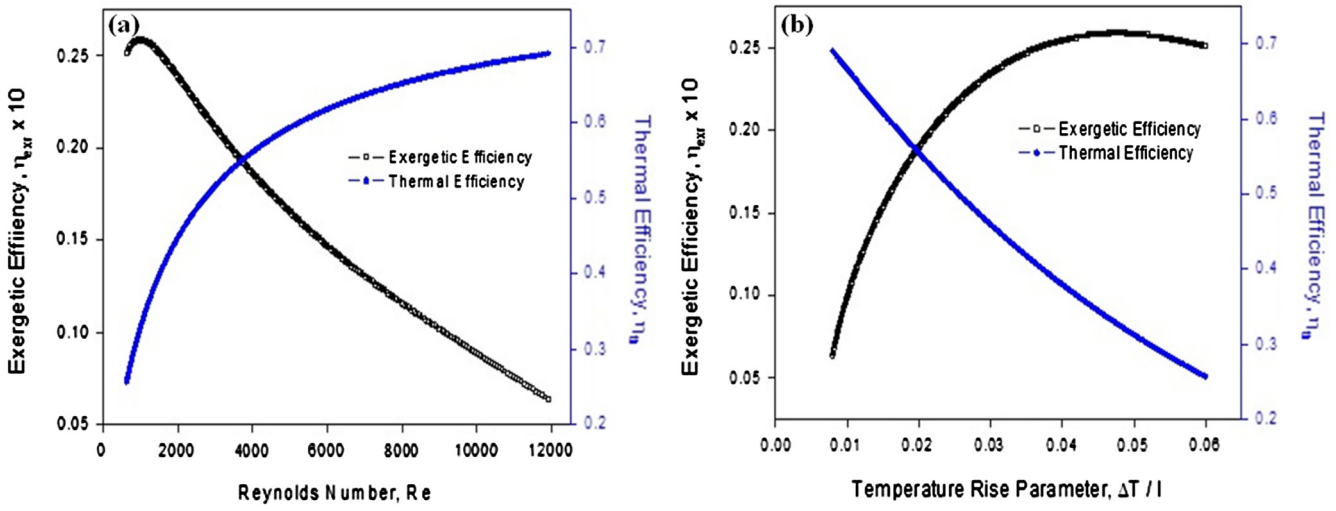

Figure 2 Variation of η_{exr} and η_{th} with (a) (Re) and (b) $[\Delta T/I]$ in an impinging jet solar air collector.

mines the formation of stagnation and wall jet region in the vicinity of the heated absorber surface from where the convection takes place. Due to increase in (D_j/D_h) the exergy delivery increases up to value of 0.065. Beyond this value the exergy delivery decreases due to interference between the jets prior to impingement over the heated surface. Also, the exergy of pump work decreases as the (D_j/D_h) increases due to decrease in the blockage area with increase in (D_j/D_h).

The effect of (X/D_h) on the η_{exr} in an impinging jet solar collector is depicted in Fig. 3b. The figure is drawn for (D_j/D_h) of 0.065, (Y/D_h) of 0.869, I of 1000 W/m^2 and varying values of (X/D_h). For $[\Delta T/I]$ below 0.011 km^2/W, the maximum value of η_{exr} is reported by (X/D_h) of 0.435 and (X/D_h) of 1.739 results in minimum value of η_{exr}. Beyond $[\Delta T/I]$ of 0.012 km^2/W the trend is reversed and the maximum η_{exr} corresponds to (X/D_h) of 1.739 and minimum for 0.435. For the values of $[\Delta T/I]$ between 0.011 and 0.012 km^2/W the maximum η_{exr} is observed for (X/D_h) of 0.869 and 1.304. Fig. 3c shows the corresponding performance plots depicting the effect of (Y/D_h) on exergetic efficiency. The figure is drawn for (D_j/D_h) of 0.065, (X/D_h) of 1.739, I of 1000 W/m^2 and varying values of (Y/D_h). The η_{exr} increases with increase in $[\Delta T/I]$ with varying values of (Y/D_h) but the exergy losses taking place through the collector dominates the optimum value of (Y/D_h). It has been observed that the value of (Y/D_h) of 0.869 performs exergetically better than other values of (Y/D_h) beyond $[\Delta T/I]$ of 0.013 km^2/W. Also, below $[\Delta T/I]$ of 0.0081 km^2/W the conventional air collector performs better than the impinging jet solar air collector.

Thus, it can be concluded that no single parameter or set of parameters result in the highest value of exergetic efficiency for the range of $[\Delta T/I]$. Thus, there is an optimum value of η_{exr} at some particular value of $[\Delta T/I]$, beyond and further of which the optimum parameters are different. Table 2 shows the enhancement in exergetic efficiency of impinging jet solar thermal collector compared to that of conventional air collector. It can be observed that the conventional solar collector presents a higher value of η_{exr} below a certain range of $[\Delta T/I]$, where the trend of maximum η_{exr} by the jet parameters is also reversed.

4.1. Design plots

The design plots have been plotted as shown in Fig. 4a–c, which presents an optimum value of jet plate parameters yielding the highest η_{exr} for different combination of $[\Delta T/I]$ and solar insolation. Fig. 4a shows the variation of (D_j/D_h) with $[\Delta T/I]$ at three different values of solar insolation. It can be seen from the figure that for all values of insolation, the jet diameter ratio of 0.065 is an optimum value for $[\Delta T/I]$ greater than 0.012 km^2/W and 0.109 for $[\Delta T/I]$ less than 0.01 km^2/W for solar radiation intensity of 1000 and is almost same for other values of solar radiation intensity. For the range of $[\Delta T/I]$ between 0.01 km^2/W and 0.012 km^2/W, an optimum value of jet diameter ratio is function of insolation and its value decreases as the insolation increases. Similarly, the design plot for (X/D_h) has been plotted as shown in Fig. 4b for different values of solar radiation intensity. It is observed that for the $[\Delta T/I]$ lower than 0.011 km^2/W, the optimum value of (X/D_h) is 0.435 and for $[\Delta T/I]$ greater than 0.012 km^2/W it is 1.739. The optimum value of (X/D_h) between these two values of $[\Delta T/I]$ is function of insolation and its value increases with increase in insolation. From Fig. 4c the optimum value of (Y/D_h) for maximum exergetic efficiency is 0.435 for $[\Delta T/I]$ less than 0.011 and 0.869 for $[\Delta T/I]$ greater than 0.013. Between $[\Delta T/I]$ of 0.011 to 0.013 the optimum (Y/D_h) is a function of insolation and observes the same trend as that of (X/D_h).

4.2. Design procedure

The study has been extended to obtain a set of jet plate parameters which would yield maximum η_{exr} for the desired value of temperature rise. This set of parameters is directly obtained from the design plots which are strong function of insolation and $[\Delta T/I]$.

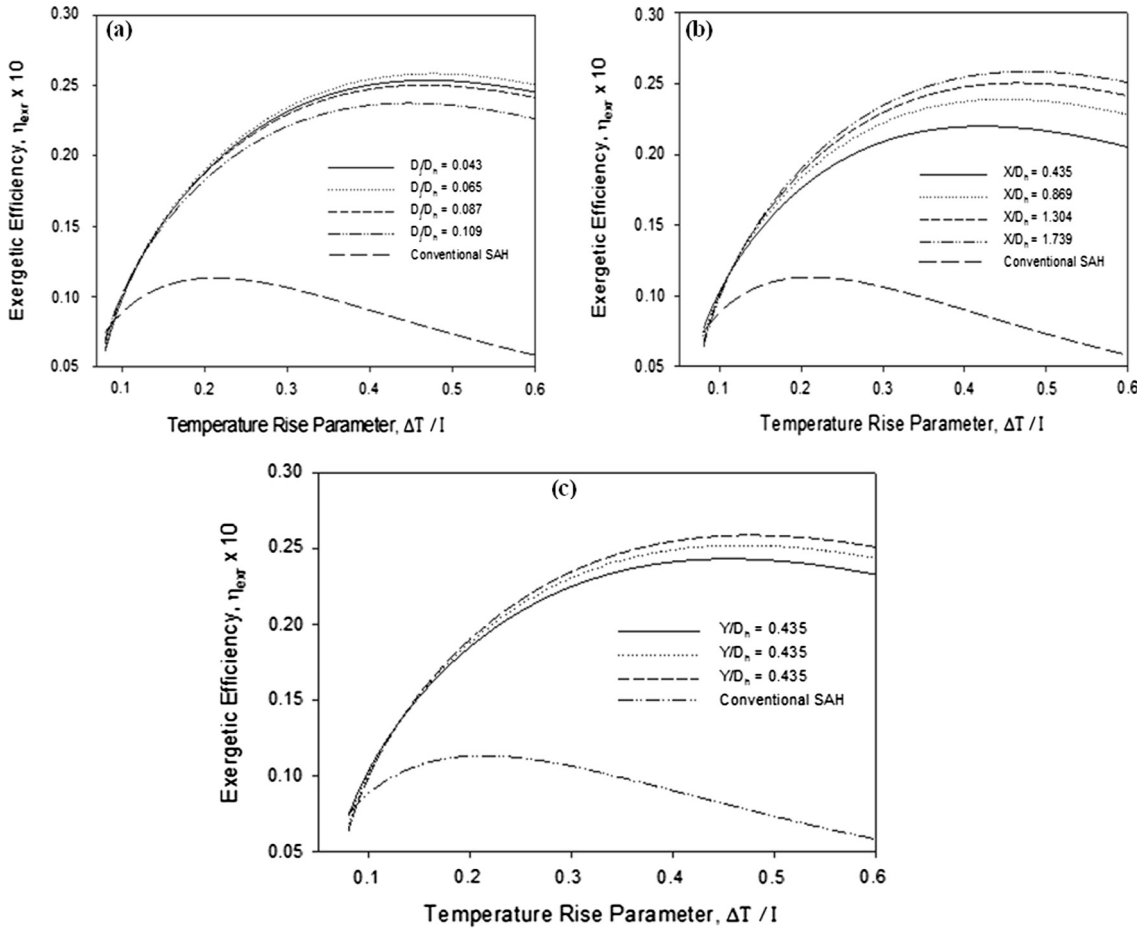

Figure 3 Exergetic efficiency as a function of (a) $[\Delta T/I]$ and jet diameter ratio, (b) $[\Delta T/I]$ and streamwise pitch ratio and (c) $[\Delta T/I]$ and spanwise pitch ratio.

Table 2 Enhancement in exergetic efficiency as a function of different jet plate parameters.

$[\Delta T/I]$ (Km^2/W)	Enhancement in exergetic efficiency (η_{exr}/η_c)											
	D_j/D_h 0.043	D_j/D_h 0.065	D_j/D_h0.087	D_j/D_h 0.109	X/D_h 0.435	X/D_h 0.869	X/D_h 1.304	X/D_h 1.739	Y/D_h 0.435	Y/D_h 0.652	Y/D_h 0.869	$\eta_{exr,c}$
0.005	0.558	0.589	0.616	0.679	0.802	0.752	0.638	0.602	0.699	0.657	0.551	0.595
0.008	0.821	0.857	0.898	0.932	1.031	0.962	0.906	0.857	0.989	0.919	0.857	0.561
0.012	1.259	1.275	1.270	1.264	1.260	1.268	1.271	1.275	1.285	1.281	1.274	0.470
0.016	1.475	1.487	1.474	1.447	1.410	1.453	1.475	1.487	1.464	1.479	1.487	0.392
0.02	1.665	1.681	1.657	1.617	1.558	1.623	1.658	1.681	1.637	1.663	1.681	0.327
0.024	1.861	1.881	1.848	1.794	1.713	1.801	1.849	1.881	1.819	1.856	1.881	0.272
0.028	2.069	2.10	2.052	1.982	1.879	1.991	2.053	2.10	2.013	2.061	2.10	0.227

The η_{exr} based upon these jet plate parameters is evaluated based upon the required energy collection rate and also enhancement in performance from that of conventional solar air collector is evaluated. An example has been cited here for illustration. For example a required temperature rise is 25 °C at solar radiation intensity of 750 W/m^2. The value of $[\Delta T/I]$ will be 0.033 km^2/W. The corresponding values of jet plate parameters would be (D_j/D_h) of 0.065, (X/D_h) of 1.739 and (Y/D_h) of 0.869. Fig. 4d is thus prepared to obtain the exergetic efficiency of impinging jet solar air collector corresponding to optimum jet parameters and that of conventional solar air collector at 25 °C of temperature rise and 750 W/m^2 of solar insolation. The η_{exr} of conventional solar air collector at $[\Delta T/I]$ of 0.033 km^2/W is 0.010. Also, the η_{exr} of impinging jet solar air collector at same $[\Delta T/I]$ and insolation comes out to be 0.024 which is 2.4 times than that of conventional solar air collector.

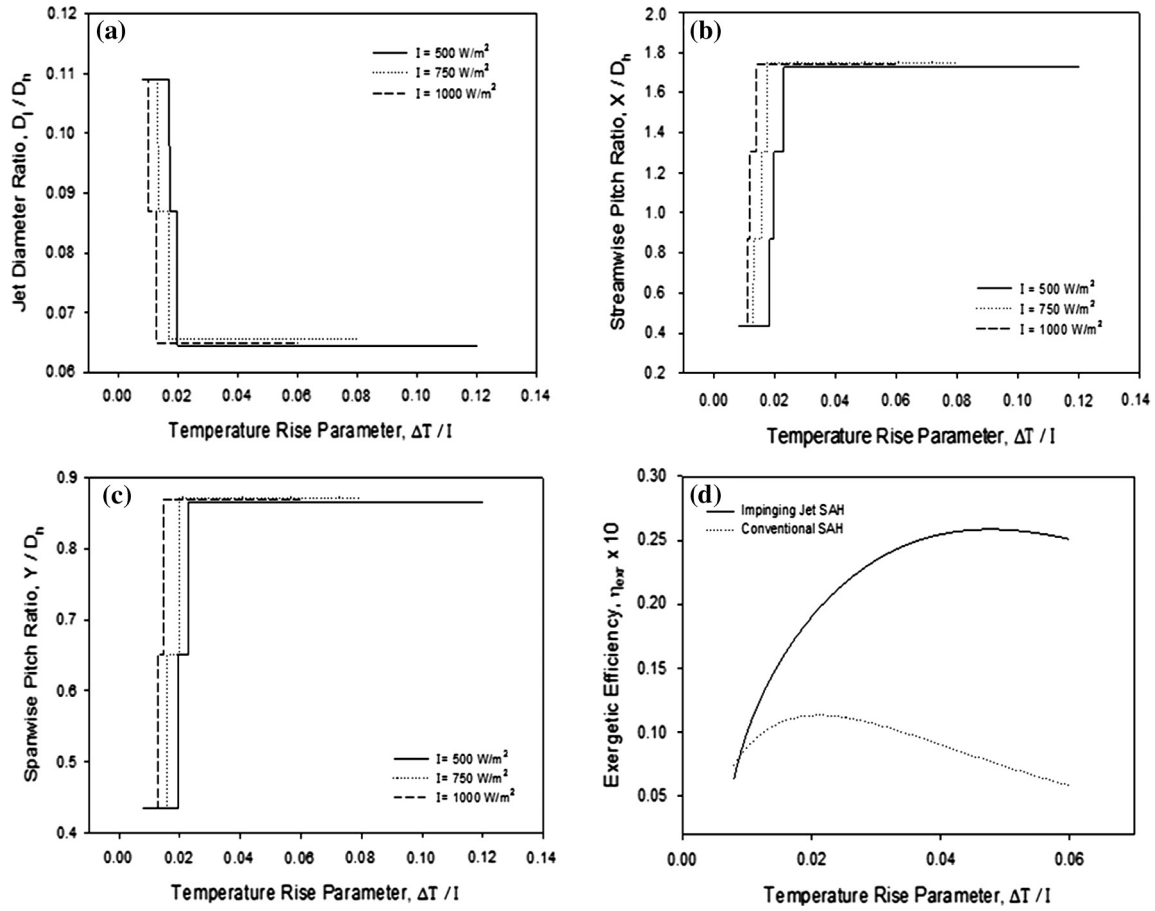

Figure 4 Optimum values of (a) Jet diameter ratio, (b) Streamwise pitch ratio, (c) Spanwise pitch ratio based upon exergetic efficiency criterion and (d) Variation of exergetic efficiency of impinging jet and conventional solar air collector with $[\Delta T/I]$.

5. Conclusions

The exergy based analysis of impinging jet solar air collector has been carried out; subject to uniform heat flux boundary conditions to study the effect of (D_j/D_h), (X/D_h) and (Y/D_h) on η_{exr}. Also, η_{exr} of the conventional solar collector has been evaluated under similar flow conditions to determine the enhancement in terms of exergetic performance.

The following salient conclusions have emerged from the study:

(a) The exergetic efficiency of impinging jet solar air collector increases at lower Reynolds number, however at high Reynolds number the exergetic efficiency decreases because the exergy of pump work required to maintain the required mass flow rate exceeds the exergy of heat gained by the collector.

(b) The exergetic efficiency increases with increase in temperature rise parameter. All the three parameters reported an increasing trend; however after certain value of temperature rise parameter constant exergetic efficiency is observed which on further increase, decreases as the exergy of pump work increases and the exergy of heat collected decreases.

(c) At lower values of temperature rise parameter, the exergy of conventional solar air collector is higher than that of impinging jet solar collector.

(d) The set of jet plate parameters viz. jet diameter ratio of 0.065, streamwise pitch ratio of 1.739 and spanwise pitch ratio of 0.869 yields the maximum exergetic efficiency above temperature rise parameter of 0.013. Below this value of temperature rise parameter the exergetic efficiency is function of jet plate parameters and solar insolation.

(e) The design plots prepared for each jet parameter at different values of solar insolation suggests different values of parameters at different temperature rise parameters. The design plots are useful to evaluate the values of system and operating parameters at desired temperature rise for maximum exergetic efficiency.

References

Alaudeen, A., Johnson, K., Ganasundar, P., Abuthahir, A.S., Srithar, K., 2014. Study on stepped type basin in a solar still. J. King Saud Univ. Eng. Sci. 26, 176–183.

Al-Dabbas, M.A., 2015. Performance evaluation of hybrid photovoltaic and thermal solar collector in Jordan. Distribut. Gen. Alter. Energy J. 30, 8–22.

Almasoud, A.H., Gandayh, H.M., 2015. Future of solar energy in Saudi Arabia. J. King Saud Univ. Eng. Sci. 27, 153–157.

Altfeld, K., Leiner, W., Febig, M., 1988. Second law optimization of flat-plate solar air heaters Part 1: the concept of net exergy flow and the modeling of solar air heaters. Sol. Energy 41, 127–132.

Bansal, N.K., 1999. Solar air heater applications in India. Renewable Energy 16, 618–623.
Bejan, A., 1988. Advanced Engineering Thermodynamics, third ed. Wiley Inderscience.
Cengel, Y.A., Boles, M.A., 2008. Thermodynamics: An Engineering Approach, sixth ed. Tata McGraw Hill.
Chauhan, R., Thakur, N.S., 2013. Heat transfer and friction factor correlations for impinging jet solar air heater. Exp. Thermal Fluid Sci. 44, 760–767.
Chauhan, R., Thakur, N.S., 2014. Investigation of the thermohydraulic performance of impinging jet solar air heater. Energy 68, 255–261.
Chauhan, R., Singh, T., Thakur, N.S., Patnaik, A., 2016. Optimization of parameters in solar thermal collector provided with impinging air jets based upon preference selection index method. Renewable Energy 99, 118–126.
Duffie, J.A., Beckman, W.A., 1974. Solar Engineering of Thermal Processes, fourth ed. Wiley.
Han, J.C., 2004. Recent studies in turbine blade cooling. Int. J. Rotating Mach. 10, 443–457.
Kandlikar, S.G., Bapat, A.V., 2007. Evaluation of jet impingement spray and microchannel chip cooling options for high heat flux removal. Heat Transfer Eng. 28, 1008–1016.
Klein, S.A., 1975. Calculation of the flat plate collector loss coefficients. Sol. Energy 17, 79–80.
Krishnananth, S.S., Murugavel, K.K., 2013. Experimental study on double pass solar air heater with thermal energy storage. J. King Saud Univ. Eng. Sci. 25, 135–140.
Kumar, R., Rosen, M.A., 2011. A critical review of photovoltaic thermal solar collectors for air heating. Appl. Energy 88, 3603–3614.
Lior, N., Zhang, N., 2007. Energy, exergy and second law performance criteria. Energy 32, 281–296.
Meola, C., 2009. A new correlation of Nusselt number for impinging jets. Heat Transfer Eng. 30, 221–228.
Panchal, H.N., 2015. Enhancement of distillate output of double basin solar still with vacuum tubes. J. King Saud Univ. Eng. Sci. 27, 170–175.
Raju, V.R., Narayana, R.L., 2018. Effect of flat plate collectors in series on performance of active solar still for Indian coastal climatic condition. J. King Saud Univ. Eng. Sci. 30 (1), 78–85.
Roger, M., Buck, R., Steinhagen, H.M., 2005. Numerical and experimental investigation of a multiple air jet cooling system for application in solar thermal receiver. ASME J. Heat Transfer 127, 682–876.
Shokouhmand, H., Jam, F., Reza, M., 2009. Optimal porosity in an air heater conduit filled with a porous matrix. Heat Transfer Eng. 30, 375–382.
Singh, S., Chander, S., Saini, J.S., 2012. Exergy based analysis of solar air heater having discrete V-down rib roughness on absorber plate. Energy 37, 749–758.
Zuckerman, N., Lior, N., 2006. Jet impingement heat transfer: physics, correlations and numerical modeling. Adv. Heat Transfer 39, 565–631.